IEEE Photonics Journal
An IEEE Photonics Society Publication

Low-Loss Graphene Waveguide Modulator for Mid-Infrared Waves

Volume 13, Number 2, April 2021

Jinwen Huang
Zhengyong Song

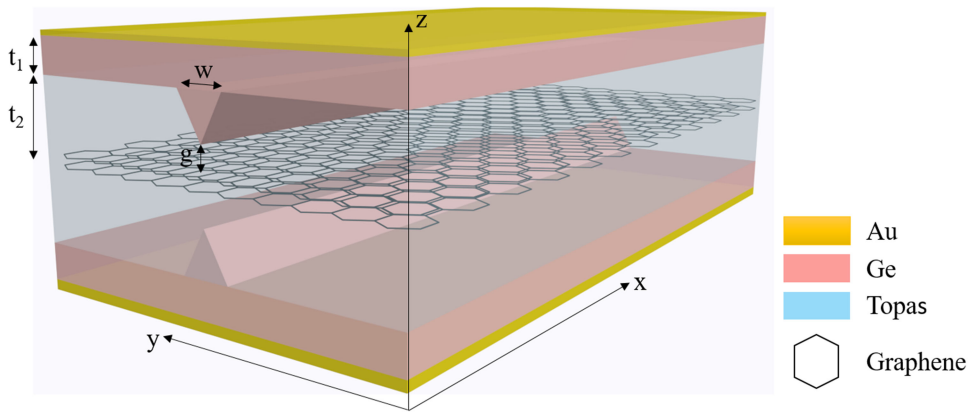

DOI: 10.1109/JPHOT.2021.3057447

Low-Loss Graphene Waveguide Modulator for Mid-Infrared Waves

Jinwen Huang[1,2] **and Zhengyong Song**[1,2]

[1]Institute of Electromagnetics and Acoustics, Xiamen University, Xiamen 361005, China
[2]Shenzhen Research Institute of Xiamen University, Shenzhen 518057, China

DOI:10.1109/JPHOT.2021.3057447

Manuscript received December 25, 2020; revised January 31, 2021; accepted February 3, 2021. Date of publication February 8, 2021; date of current version February 23, 2021. This work was supported in part by the National Natural Science Foundation of China under Grant 11974294 and in part by the Guangdong Basic and Applied Basic Research Foundation under Grant 2020A1515010375. Corresponding author: Zhengyong Song (e-mail: zhysong@xmu.edu.cn).

Abstract: Graphene waveguide plays an important role in modulating optical signal. But it is hard to make a tradeoff between low propagating loss and high field confinement. Here, we propose a bilayer graphene waveguide in a thin topas film and a high refractive index material-germanium cladded with thin metallic film. The influences of structural parameter and chemical potential of graphene are studied to optimize the dimension and working mode. Simulation reveals that our structure can make a balance between high figure of merit (FOM) and low propagation loss, and it reaches a high modulation depth of 2.5 dB/μm. The design can work with FOM over 200, propagation loss lower than 0.2 dB/μm, and propagation length beyond 30 μm in a wide band from 6 THz to 18 THz. Compared with previous graphene waveguides, our structure operates from terahertz band to mid-infrared band, and it has longer propagation length due to the existence of bilayer graphene. Besides, benefiting from the thin metallic film, our structure can be integrated on chip.

Index Terms: Graphene, modulator, plasmonics, waveguide.

1. Introduction

Graphene is a two-dimensional carbon material with great potentialities for its extraordinary properties in the fields of thermology [1], [2], chemistry [3], [4], electricity [5], and optics [6]. Its unique electrical and optical features are inherently caused by the distinctive Dirac cone band structure, which means graphene owns linear energy dispersion with zero bandgap energy [7], [8]. Another advantage of graphene is that it is compatible with complementary metal oxide semiconductor (CMOS) process, so it is significant to carry out research on photoelectric devices with graphene [9]. Compared with noble metals, graphene possesses ultrahigh carrier mobility of 2×10^5 cm$^2/(VS)$, and this character make it possible to modulate optical signal flexibly. Meanwhile, graphene's optical and electrical properties can be easily tuned by bias voltage. Therefore, people can manually control the status of modulator based on graphene switch between on and off [10]–[14].

Graphene plasmonic waveguide (GPWG) has been widely used in modern communication technology, and scientists have already improved some feasible schemes to achieve optical signal modulation or detection [15]–[20]. As a result of the interaction between wave and inside materials of waveguide when wave travels in the waveguide structure, optical performances of waveguide-based detector, absorber and modulator can be greatly tuned by chemical doping and

external bias voltage owning to the flexible adjustability of graphene [21]–[24]. High-performance light switch and sensor can also be obtained with reasonable control of scattering rate, thanks to high free electron concentration and the introduction of graphene. In 2013, Horvath *et al.* verified a silicon waveguide based on graphene by simulation and experiment [25]. The nonlinear coefficient is generated by heating graphene through PMMA layer, and the maximum modulation depth (MD) is 2.7 dB/μm. The difference between simulation and measured results is within a reasonable range, but it can only modulate light with input power around 15 mW. In 2014, Kim *et al.* experimentally demonstrated a graphene rectangular waveguide [26]. By heating graphene, carrier velocity inside graphene is changed and then the intensity of optical signal is modulated. It is found that MD of the device can achieve 10 dB/μm. However, limited by the heating speed, the response time of the device is 10 ms, and the energy consumption of switching between on and off is large. In 2015, Ansell *et al.* experimentally studied a 100 μm waveguide composed of graphene and metal [27]. Experimental results show that this device owns a MD over 0.03 dB/μm. In 2016, Liu *et al.* demonstrated a cylindrical waveguide wrapped with graphene [28]. This structure can transmit multiple eigenmodes in the mid-infrared band, but propagation length of high-order modes is much smaller than that of the fundamental mode. It is evident when Fermi level is higher. The maximum propagation length of the device is less than 8 μm. The reason of this phenomenon is that electromagnetic eigenmodes are distributed near the surface of a cylinder and it makes the contact area very large between wave and graphene, so all eigenmodes suffers high loss. In 2017, Doust *et al.* showed a bilayer graphene waveguide [29]. Two graphene sheets are separated by low refractive index material. At 30 THz, propagation length of the waveguide is 4 μm. When chemical potential is adjusted to 0.8 eV, electric filed distribution of eigenmode has a penetration distance of 300 μm in the longitudinal direction. In 2018, Cai *et al.* conducted an in-depth study on a rectangular dielectric waveguide [30]. This device can modulate TE mode with a MD of 0.25 dB/μm by changing chemical potential, and at the same time TM mode is transmitted with minimal loss, so TM mode can be transmitted over 150 μm. In 2019, Hu *et al.* designed an ultra-compact silicon strip waveguide that can modulate both phase and intensity, and verified it in simulation [31]. This structure can be used to control TE mode with a MD of 0.3 dB/μm and a maximum 0.8π change in phase of the signal light. In 2019, Luan *et al.* proposed a waveguide structure loaded with four graphene sheets on the surface [32]. Electromagnetic energy is confined by using silicon and silver. MD of the device is 0.45 dB/μm, and the value of figure of merit (FOM) does not exceed 12 after parameter optimization. In 2020, Heydari *et al.* demonstrated a waveguide coated with graphene [33], both theoretical and numerical results showed that their design owns a tinny FOM value no more than 30. In 2020, Cai *et al.* proposed a waveguide modulator composed of a silver cylinder and graphene sandwich structure [34]. Benefiting from the strong interaction between graphene and wave and the strong confinement of electromagnetic wave, the normalized effective mode area is less than 0.015, and the maximum propagation length is 21 μm. In this work, we propose a hybrid plasmonic waveguide with bilayer graphene embedded in the middle of the configuration. After parameter optimization, it is verified that the maximum MD of this structure is 2.5 dB/μm. In the wide band of 6–18 THz, propagation length of the fundamental and higher-order modes is more than 25 μm, and the maximum FOM value can exceed 200.

2. Design and Method

Fig. 1 shows the diagrammatic sketch of the designed three-dimensional graphene plasmonic waveguide. Bilayer graphene with the distance of 10 nm is inserted in the middle of the low refractive index material (topas). The thickness of topas is $2t_2$. Two germanium triangular prisms with a bottom edge width w are located at the top and bottom of topas. The distance between the triangular prism and graphene is *g*. The cladding material with the thickness of t_1 is germanium with high refractive index to limit the area of field pattern. To prevent electromagnetic wave spread out of the device, two gold films are deposited on the top and bottom of the design. The relative dielectric permittivity of topas and germanium is taken as 2.35 and 16 [35], [36]. The relative

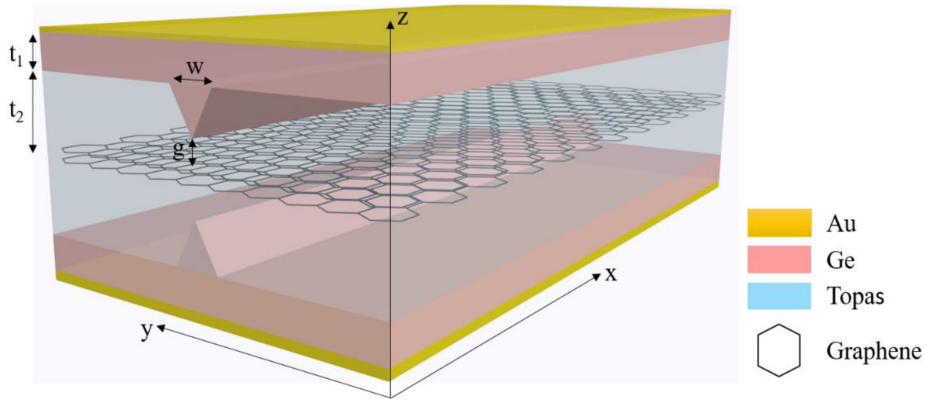

Fig. 1. Three-dimensional schematic of the proposed graphene plasmonic waveguide.

dielectric permittivity of gold is described by a Drude model $\varepsilon_{Au} = 1 - \omega_p^2/\omega(\omega + i\Gamma)$ with plasma frequency $\omega_p = 1.37 \times 10^{16}$ rad/s and collision frequency $\Gamma = 1.2 \times 10^{14}$ rad/s [37].

As for graphene, it can be modeled as a two-dimensional surface with regularly changing conductivity described by Kubo formula [34], [38]. This method not only reduces the computational complexity, but also simplifies the model. The following (1), (2), and (3) are employed to describe the conductivity of graphene.

$$\sigma_g(\omega, E_f, \tau, T) = \sigma_{\text{intra}}(\omega, E_f, \tau, T) + \sigma_{\text{inter}}(\omega, E_f, \tau, T) \tag{1}$$

$$\sigma_{\text{intra}} = \frac{2ie^2 T k_B}{\pi\hbar^2(\omega + i\tau^{-1})} \ln\left[2\cosh\left(\frac{E_f}{2Tk_B}\right)\right] \tag{2}$$

$$\sigma_{\text{inter}} = \frac{e^2}{4\hbar}\left[\frac{1}{2} + \frac{1}{\pi}\arctan\left(\frac{\hbar\omega - 2E_f}{2Tk_B}\right) - \frac{i}{2\pi}\ln\frac{(\hbar\omega + 2E_f)^2}{(\hbar\omega - 2E_f)^2 + (2Tk_B)^2}\right] \tag{3}$$

ω represents the angular frequency of electromagnetic wave, E_f is the chemical potential of graphene, τ is the relaxation time of graphene. Here, τ is 1.2 ps. $\hbar$ is the reduced Planck constant, k_B is the Boltzmann constant, and T is the temperature. Temperature is set as 300 K during the simulation. Surface current would occur when incident wave interacts with graphene and surface current density can be described as $\vec{J} = \sigma\vec{E}$. Conductivity can be tuned by chemical doping or applied voltage. It's worthy to note that Kubo formula can be simplified in some special regions. When Fermi level has a moderate value $-\frac{\hbar\omega}{2} < E_f < \frac{\hbar\omega}{2}$, only incident photons can excite electrons by interband transition, which results in a large light absorption. If Fermi level satisfies the relationship $E_f < -\frac{\hbar\omega}{2}$, there is nearly no electron in the interband transition, which leads to high optical transmission. And conversely, when Fermi level meets the requirement of $E_f > \frac{\hbar\omega}{2}$, there is no more room in conduction band for more electrons, and the interband transition is inadmissibility, resulting in higher light transmission [39].

In order to calculate the modal properties of this structure precisely, finite element method (commercial softwares-COMSOL Multiphysics) is applied. Through this software, we can obtain real and imaginary parts of effective mode index of graphene plamonic waveguide. Then, propagation length of surface plasmon polariton (L_{SPP}), attenuation coefficient (α), FOM, and MD are introduced to evaluate the performance of this device. And these physical quantities are defined as follows:

$$N_{eff} = \frac{\beta\lambda_0}{2\pi} \tag{4}$$

$$L_{spp} = \frac{\lambda}{4\pi\,\text{Im}(N_{eff})} \tag{5}$$

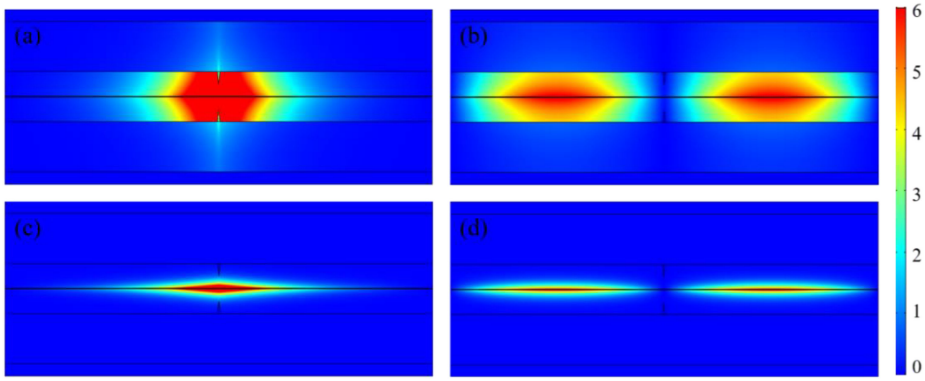

Fig. 2. Intensity distributions of electric fields of fundamental mode ((a) and (c)) and second-order mode ((b) and (d)) at E_f= 0.1 eV. (a) and (b) Electric field distributions at 9 THz. (c) and (d) Electric field distributions at 18 THz.

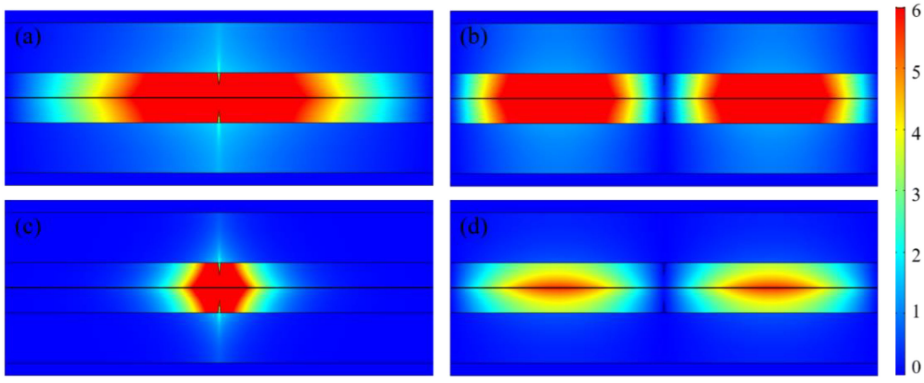

Fig. 3. Intensity distributions of electric fields of fundamental mode ((a) and (c)) and second-order mode ((b) and (d)) at E_f= 0.9 eV. (a) and (b) Electric field distributions at 9 THz. (c) and (d) Electric field distributions at 18 THz.

$$\alpha = \frac{10\mathrm{Im}(N_{eff})4\pi}{\lambda_0 \ln 10} \tag{6}$$

$$FOM = \frac{\mathrm{Re}(N_{eff})}{\mathrm{Im}(N_{eff})} \tag{7}$$

$$MD = \alpha(OFF) - \alpha(ON) \tag{8}$$

L_{SPP} is used to describe the maximum propagation length of mode, and α is corresponding to L_{spp} which present propagation loss per micron. In addition, FOM can be made available for structure's quality factor.

3. Results and Discussions

In practical applications, electromagnetic waves enter or get out our structure at a specific angle by means of a Bragg grating coupler. After that, graphene plasmonic waveguide can confine incident wave in a bitty area and enhance wave-matter interaction. With the help of graphene, we can control the intensity of incident wave by altering chemical potential. When chemical potentials are set as 0.1 eV and 0.9 eV, the corresponding intensity distributions of electric filed are shown in Fig. 2 and Fig. 3. Figs. 2(a) and 2(b) are obtained at the frequency of 9 THz, and Figs. 2(c) and 2(d) are obtained at the frequency of 18 THz. In Fig. 3, the corresponding field distributions are simulated at chemical potential $E_f = 0.9$ eV. Whether it is the fundamental mode or the second-order mode,

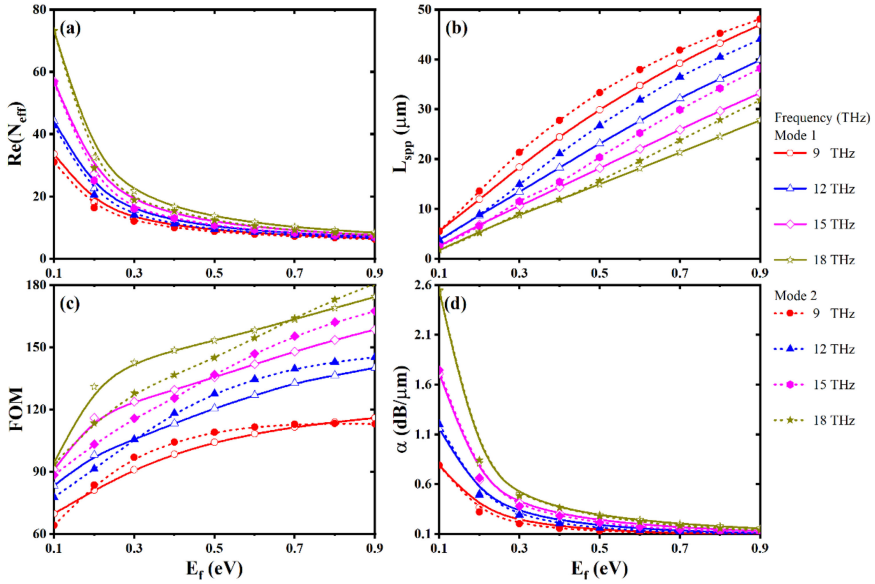

Fig. 4. Effective mode refractive index (a), propagation length (b), FOM (c), and attenuation coefficient (d) of fundamental mode and second-order mode varies with chemical potentials at different frequencies. The used structural parameters are $t_1 = 600$ nm, $t_2 = 400$ nm, $w = 200$ nm, and $g = 140$ nm.

electric filed is always confined in low refractive index material-topas. Comparing Fig. 2 with Fig. 3, we can draw a conclusion that graphene with the lower chemical potential has a weaker interaction with input wave, so the area of field distribution in Fig. 2 seems smaller than that in Fig. 3. And benefiting from triangular germanium, the normalized pattern area of the fundamental mode is much smaller than that of the second-order mode.

Fig. 4 shows the modulation function of our design. The interaction between graphene and incident wave is weak when chemical potential is low, which brings a significant attenuation and a shorter propagation length. At the same time, FOM is smaller even much smaller than 100 due to the faint growth of real part and strong growth of imaginary part of N_{eff}. When chemical potential is turned up to 0.9 eV, electromagnetic wave can transmit at a minute loss and FOM can reach a tremendous value. Two distinct propagation characteristics of electromagnetic waves predict that this device can be treated as a modulator with an excellent MD of 2.5 dB/μm. By observing solid and dashed lines at the same frequency, it is noticed that this device is capable to manipulate multimode for the fundamental mode and the second-order mode, and both of them perform very similarly. Besides, at high frequencies, there is a more pronounced contrast between high and low chemical potentials, so this device can modulate high-frequency electromagnetic wave more efficiently.

In order to search out the optimum structure parameter and optimize the performance, parameter sweepings are performed on several structural parameters of this device. Fig. 5 presents the effect of germanium thickness (t_1) on our device. At the same frequency, whether it is fundamental mode or second-order mode, the thicker the germanium, the larger the real and imaginary parts of effective mode refractive index, and the smaller the propagation length. But the value of FOM is almost unchanged. This is because the thinner the germanium, the more energies of electromagnetic wave penetrate into the metal surface, resulting in a greater loss. With the increase of frequency, L_{spp} decreases in Fig. 5(b) and FOM increases quickly in Fig. 5(c). The phenomenon appears in Fig. 5(b) can be explained in two ways, and one of the reasons is shown in Fig. 5(d). High-frequency signal possesses stronger interaction with graphene, and it causes imaginary part of N_{eff} increase. Another more important reason is that L_{spp} is strongly influenced by wavelength. As frequency increases from 6 THz to 18 THz, the corresponding wavelength decreases from 50 μm to 16.7 μm.

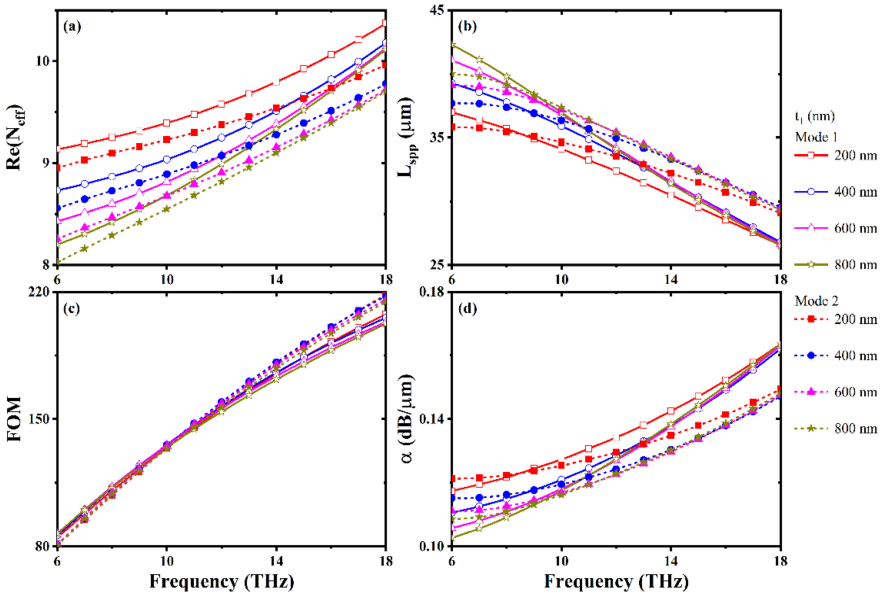

Fig. 5. Effective mode refractive index (a), propagation length (b), FOM (c), and attenuation coefficient (d) of fundamental mode and second-order mode changes with frequency of incident wave when t_1 takes different values. The used chemical potential is 0.9 eV.

In Fig. 5(d), although the curves appear to be an obvious upward trend, the value of α stays at a very low level, and electromagnetic waves do not transmit a micron and lose up to 3.6% of their energy. And benefiting from bilayer graphene, propagation length of this device is still longer than that of many other devices. When the thickness of germanium is more than 600 nm, the performance of the device is almost unaffected. Therefore, the thickness of germanium is chosen to be 600 nm. Another advantage of bilayer graphene is that transport properties of higher-order and fundamental modes are very similar, which is difficult to achieve in single-layer graphene devices.

Fig. 6 is the results after parameter sweep of topas thickness (t_2). From electric field distributions in Figs. 2 and 3, we can draw a conclusion that most energy of electromagnetic wave is concentrated in the toaps layer, so the thickness of topas has a significant effect on the device. Take the point of 12 THz for example, as the topas layer becomes thicker, real part of effective mode refractive index increases from 6.6 to 8.1 and imaginary part decreases, so propagation length increases from 36 μm to 42 μm. Unfortunately, due to the insufficient variation of real part, the value of FOM decreases from 150 to 140 and it becomes more obvious as frequency increases. Thus, we had to make a tradeoff between L_{spp} and FOM. For a balance between propagation length and FOM, here we choose a topas thickness as 400 nm.

As shown in Fig. 1, there is a germanium triangular prism in our structure. Its main function is to adjust fundamental mode in the waveguide structure, so we will analyze the influence of the geometry of germanium triangular prism on propagation performance of fundamental mode. Under the condition that the thickness of the topas layer is fixed as 400 nm, the fundamental mode is regulated by changing the length of W and the distance g between germanium triangular prism and the nearest graphene layer. Fig. 7 shows the influence of W on propagation performance of the fundamental mode. Firstly, it is noted that no matter how the value of W changes, propagation characteristic curves of the second-order mode are almost unaffected while the fundamental mode is significantly regulated. At the same frequency, the smaller the value of W, the smaller the real and imaginary parts of effective mode refractive index. The change rate of real part is greater than that of imaginary part, so the corresponding L_{spp} and FOM values will increase. A proper reduction of W value is beneficial to electromagnetic wave propagation in this graphene plasmonic waveguide. Therefore, we take a W value of 200 nm.

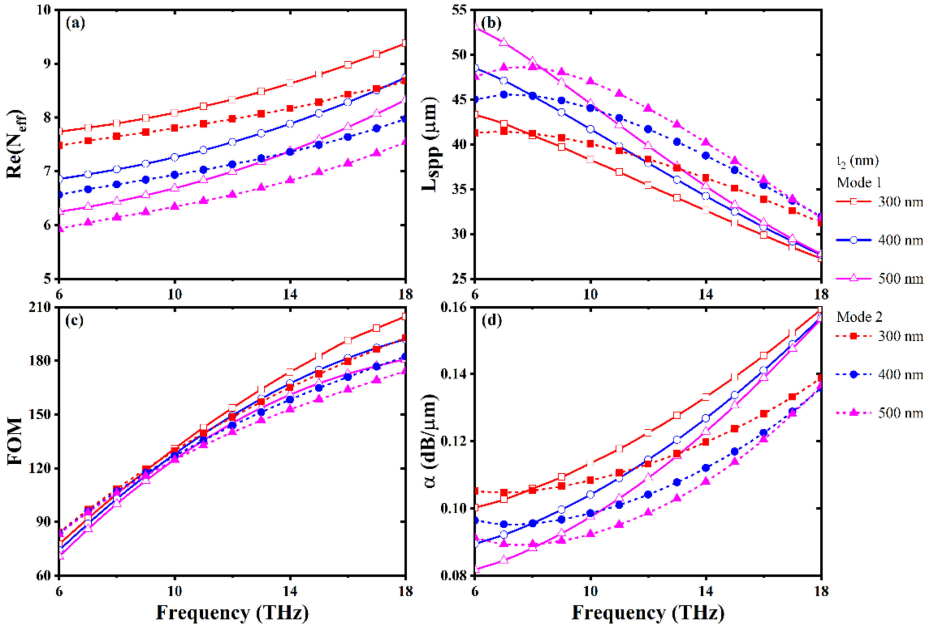

Fig. 6. Effective mode refractive index (a), propagation length (b), FOM (c), and attenuation coefficient (d) of fundamental mode and second-order mode changes with frequency of incident wave when t_2 takes different values. The used chemical potential is 0.9 eV.

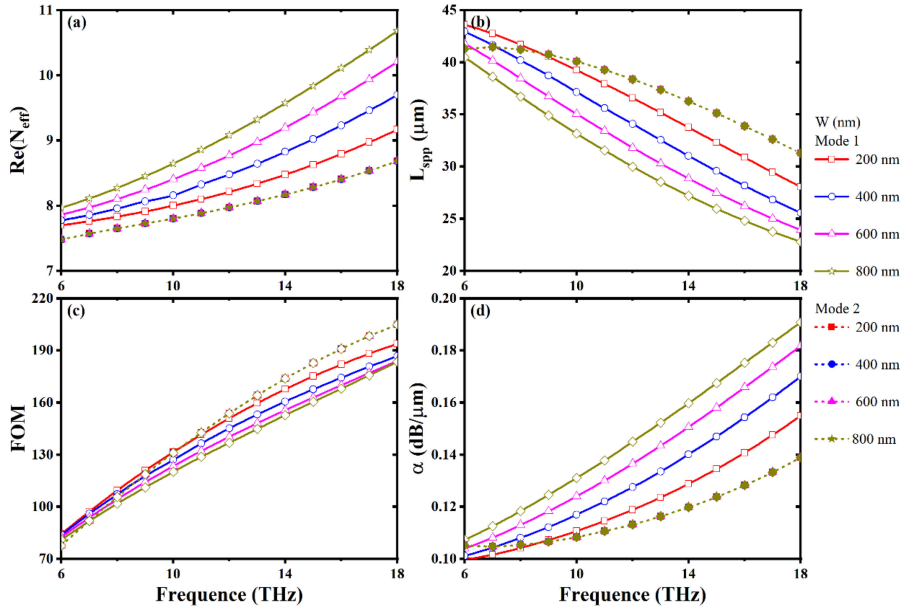

Fig. 7. Effective mode refractive index (a), propagation length (b), FOM (c), and attenuation coefficient (d) of fundamental mode and second-order mode changes with frequency of incident wave when W takes different values. The used chemical potential is 0.9 eV.

The curves in Fig. 8 describe the effect of geometry parameter g on device performance. The results clearly tell that the variable g only affects the fundamental mode. Figs. 8(a) and 8(c) show that real part and attenuation coefficient of effective mode refractive index are slightly affected when the value of g exceeds 140 nm. Propagation length and FOM are lower when the value is 90 nm (red curve), so here we determine that the value of g is 140 nm.

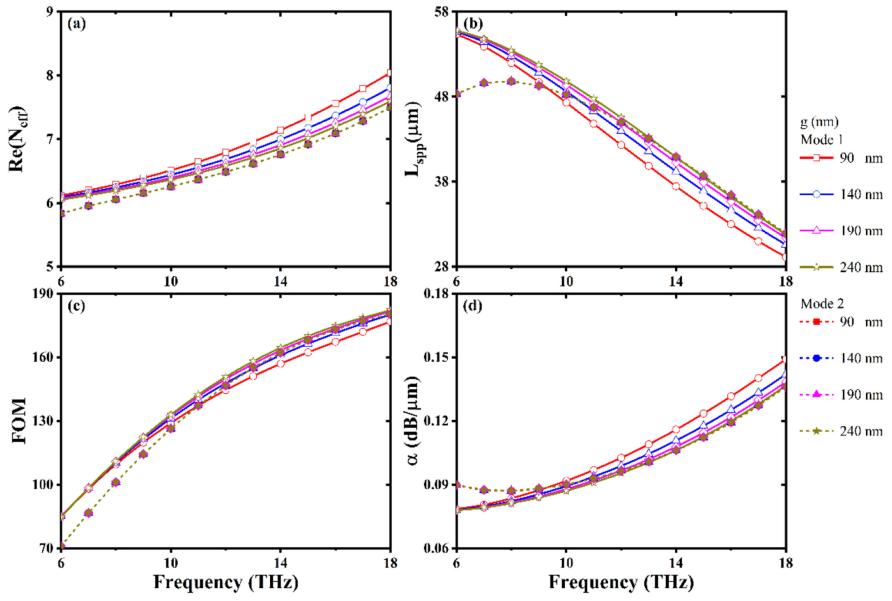

Fig. 8. Effective mode refractive index (a), propagation length (b), FOM (c), and attenuation coefficient (d) of fundamental mode and second-order mode changes with frequency of incident wave when g takes different values. The used chemical potential is 0.9 eV.

TABLE 1
A Comparison Between Previous Works and Our Work

References	Grapene layers	Frequency (THz)	FOM	Propagation length (μm)	Modulation depth (dB/μm)
[27]	1	200	-	7.68	0.03
[28]	1	42.86	30	8	2.17
[29]	2	47.62	-	3	1.45
[30]	4	182-207	2772	1.023	0.22
[31]	2	150-229	211	28.8	0.32
[32]	4	200	10.9	85	0.523
[33]	1	10-50	30	0.23	0.22
[34]	2	200	-	20	0.217
This work	2	8-18	214	52	2.5

4. Conclusion

After a series of parameter optimization, the thickness of gold is 100 nm, the thickness of germanium is 600 nm, the thickness of topas is 400 nm, the length of triangle bottom edge is 200 nm, and the distance of triangle vertex from nearest graphene layer is 140 nm. In this condition, this waveguide possesses excellent performance when working in terahertz band and mid-infrared band. When chemical potential of graphene is regulated in the range of 0.1 eV-0.9 eV, this device can obtain a maximum modulation depth of 2.5 dB/μm at 18 THz. If chemical potential of graphene is fixed at 0.9 eV and frequency is changed in the range of 6–10 THz, we can keep propagation length of electromagnetic wave above 25 μm and the maximum FOM value can exceed 200. Besides, effective mode area of the fundamental mode is reduced by adding a germanium triprism with a high dielectric constant, and imaginary part of effective mode factor of the intrinsic mode is greatly reduced by introducing bilayer graphene. These characteristics enable this device to be used as a light modulator or a platform in an integrated optical circuit. Comparing with previous reported graphene-on-waveguide designs [40], [41], our present design takes advantages of higher propagation loss and greater MD for both fundamental mode and higher-order eigenmodes. The data in the Table 1 is the best point in some cited papers. These references reveal that it is difficult to make a tradeoff between FOM, L_{SPP} and MD, and there is still great potential to explore modulating ability of graphene dielectric waveguide in the terahertz, infrared or telecommunication band. This configuration can be manufactured by using the existing technology. A 100 nm thick Au film is deposited on germanium layer by magnetron sputtering. Germanium is etched with a mixture of nitric acid and hydrofluoric to form a triangular germanium. Then, ring-opening metathesis polymerization of cycloolefins is carried out with a catalyst to obtain topas. Bilayer graphene can be prepared by Hummers method.

Disclosures: The authors declare that there are no conflicts of interest related to this article.

References

[1] A. K. Geim and K. S. Novoselov, "The rise of graphene," *Nat. Materials*, vol. 6, no. 3, pp. 183–191, 2007.
[2] C. G. Lee, X. D. Wei, J. W. Kysar, and J. Hone, "Measurement of the elastic properties and intrinsic strength of monolayer graphene," *Science*, vol. 321, no. 5887, pp. 385–388, 2018.
[3] A. C. Ferrari *et al.*, "Raman spectrum of graphene and graphene layers," *Phys. Rev. Lett.*, vol. 97, no. 18, 2006, Art. no. 187401.
[4] S. Q. Zhao *et al.*, "Cross-plane transport in a single-molecule two-dimensional van der waals heterojunction," *Sci. Adv.*, vol. 6, no. 22, 2020, Art. no. eaba6741.
[5] A. H. C. Neto, F. Guinea, N. M. R. Peres, K. S. Novoselov, and A. K. Geim, "The electronic properties of graphene," *Rev. Mod. Phys.*, vol. 81, no. 1, pp. 109–162, 2009.
[6] S. Stankovich *et al.*, "Graphene-based composite materials," *Nature*, vol. 442, no. 7100, pp. 282–286, 2006.
[7] C. Y. Zhong, J. Y. Li, and H. T. Lin, "Graphene-based all-optical modulators," *Front. Optoelectron.*, vol. 13, no. 2, pp. 114–128, 2020.
[8] S. J. Zhang, Z. W. Li, and F. Xing, "Review of polarization optical devices based on graphene materials," *Int. J. Mol. Sci.*, vol. 21, no. 5, 2020, Art. no. 1608.
[9] Y. H. Ding *et al.*, "Ultra-compact integrated graphene plasmonic photodetector with bandwidth above 110 GHz," *Nanophotonics*, vol. 9, no. 2, pp. 317–325, 2020.
[10] K. Zheng *et al.*, "Ultra-compact, low-loss terahertz waveguide based on graphene plasmonic technology," *2D Materials*, vol. 7, no. 1, 2020, Art. no. 015016.
[11] M. Y. Su *et al.*, "Broadband graphene-on-silicon modulator with orthogonal hybrid plasmonic waveguides," *Nanophotonics*, vol. 9, no. 6, pp. 1529–1538, 2020.
[12] P. J. Wang *et al.*, "Plasmonic Feynman gate based on suspended graphene nano-ribbon waveguides at THz wavelengths," *IEEE Photon. J.*, vol. 11, no. 3, Jun. 2019, Art. no. 4801109.
[13] J. Zhang, X. Wei, M. Premaratne, and W. Zhu, "Experimental demonstration of an electrically tunable broadband coherent perfect absorber based on a graphene-electrolyte-graphene sandwich structure," *Photon. Res.*, vol. 7, no. 8, pp. 868–874, 2019.
[14] J. Zhang *et al.*, "Dynamic scattering steering with graphene-based coding metamirror," *Adv. Opt. Materials*, vol. 8, no. 19, 2020, Art. no. 2000683.
[15] L. A. Shoramin and D. V. Thourhout, "Graphene modulators and switches integrated on silicon and silicon nitride waveguide," *IEEE. J. Sel. Topics Quantum Electron.*, vol. 23, no. 1, Jan./Feb. 2017, Art. no. 3600107.
[16] J. Petersen, J. Volz, and A. Rauschenbeurel, "Chiral nanophotonic waveguide interface based on spin-orbit interaction of light," *Science*, vol. 346, no. 6205, pp. 67–71, 2014.

[17] B. H. Fakhar, M. Ghazialsharif, and M. S. Abrishamian, "Graphene hybrid waveguide stimulation using a photoconductive terahertz generator," *Opt. Lett.*, vol. 45, no. 8, pp. 2407–2410, 2020.
[18] M. Soltani, T. Branch, and T. Iran, "A graphene based bimetallic plasmonic waveguide to increase photorefractive effect," *Wave Random Complex*, vol. 2, no. 4, 2020, Art. no. 1745030.
[19] J. S. Guo *et al.*, "High-performance silicon-graphene hybrid plasmonic waveguide photodetectors beyond 1.55 μm," *Light-Sci. Appl.*, vol. 9, no. 1, pp. 1–11, 2020.
[20] X. M. Wang, Z. Z. Cheng, K. Xu, H. K. Tsang, and J. B. Xu, "High-responsivity graphene/silicon-heterostructure waveguide photodetectors," *Nat. Photon.*, vol. 7, no. 11, pp. 888–891, 2013.
[21] X. Luo *et al.*, "A tunable dual-band and polarization-insensitive coherent perfect absorber based on double-layers graphene hybrid waveguide," *Nanoscale Res. Lett.*, vol. 14, no. 1, 2019, Art. no. 14337.
[22] A. Q. Zhang, W. B. Lu, Z. G. Liu, B. Wu, and H. Chen, "Flexible and dynamically tunable attenuator based on spoof surface plasmon polaritons waveguide loaded with graphene," *IEEE Trans. Antennas Propag.*, vol. 67, no. 8, pp. 5582–5589, Aug. 2019.
[23] G. R. Sui, J. Wu, Y. H. Zhang, C. H. Yin, and X. M. Gao, "Microcavity-integrated graphene waveguide: A reconfigurable electro-optical attenuator and switch," *Sci. Rep.*, vol. 8, 2018, Art. no. 12445.
[24] B. Wu, Y. H. Zhang, H. R. Zu, and W. B. Lu, "Tunable grounded coplanar waveguide attenuator based on graphene nanoplates," *IEEE Microw. Wireless Compon. Lett.*, vol. 29, no. 5, pp. 330–332, May 2019.
[25] C. Horvath, D. Bachman, R. Indoe, and V. Van, "Photothermal nonlinearity and optical bistability in a graphene-silicon waveguide resonator," *Opt. Lett.*, vol. 38, no. 23, pp. 5036–5039, 2013.
[26] J. T. Kim, H. Choi, Y. J. Yu, K. H. Chung, and C. G. Choi, "Graphene-based photonic waveguide devices," in *Proc. Conf. Integr. Opt.: Devices, Materials, Technol. XVIII*, 2014, vol. 8988, Art. no. 898802.
[27] D. Ansell, I. P. Radko, Z. Han, F. J. Rodriguez, S. I. Bozhevolnyi, and A. N. Grigorenko, "Hybrid graphene plasmonic waveguide modulators," *Nat. Commun.*, vol. 6, no. 1, pp. 839–843, 2015.
[28] J. P. Liu *et al.*, "Analysis of mid-infrared surface plasmon modes in a graphene-based cylindrical hybrid waveguide," *Plamonics*, vol. 11, no. 3, pp. 703–711, 2016.
[29] S. K. Doust, V. Siahpoush, and A. Asgari, "The tunability of surface plasmon polaritons in graphene waveguide structures," *Plasmonics*, vol. 12, no. 5, pp. 1633–1639, 2017.
[30] K. Su. Cai *et al.*, "TM-pass polarizer based on multilayer graphene polymer waveguide," *Opto-Electron. Lett.*, vol. 14, no. 3, pp. 0181–0184, 2018.
[31] X. Hu, Y. G. Zhang, D. G. Chen, X. Xiao, and S. H. Yu, "Design and modeling of high efficiency graphene intensity/phase modulator based on ultra-thin silicon strip waveguide," *J. Lightw. Techonol.*, vol. 37, no. 10, pp. 2284–2292, May 2019.
[32] J. Y. Luan *et al.*, "Design and optimization of a graphene modulator based on hybrid plasmonic waveguide with double low-index slots," *Plamonsics*, vol. 14, no. 1, pp. 133–138, 2019.
[33] M. B. Heydari and M. H. V. Samiei, "An analytical study of magneto-plasmons in anisotropic multi-layer structures containing magnetically biased graphene sheets," *Plasmonics*, vol. 15, no. 4, pp. 1183–1198, 2020.
[34] M. Cai, S. L. Wang, Z. H. Liu, Y. D. Wang, T. Han, and H. X. Liu, "Graphene electro-optical switch modulator by adjusting propagation length based on hybrid plasmonic waveguide in infrared band," *Sensor*, vol. 20, no. 10, 2020, Art. no. 2864.
[35] P. D. Cunningham *et al.*, "Broadband terahertz characterization of the refractive index and absorption of some important polymeric and organic electrooptic materials," *Appl. Phys. Lett.*, vol. 109, no. 69, 1996, Art. no. 2321.
[36] H. H. Li, "Refractive index of silicon and germanium and its wavelength and temperature derivatives," *J. Phys. Chem.*, vol. 9, no. 3, pp. 561–658, 1993.
[37] N. Liu *et al.*, "Plasmonic analogue of electromagnetically induced transparency at the drude damping limit," *Nat. Materials*, vol. 8, no. 9, pp. 758–762, 2009.
[38] J. Y. Luan *et al.*, "Design and optimization of a graphene modulator based on hybrid plasmonic waveguide with double low-index slots," *Plamonsics*, vol. 14, no. 1, pp. 133–138, 2019.
[39] J. Y. Jiao *et al.*, "Optimization of graphene-based slot waveguides for efficient modulation," *IEEE. J. Sel. Topics Quantum Electron.*, vol. 20, no. 2, Mar./Apr. 2020, Art. no. 8200705.
[40] T. H. Xiao, Z. Cheng, and K. Goda, "Graphene-on-silicon hybrid plasmonic-photonic integrated circuits," *Nanotechnology*, vol. 28, no. 24, 2017, Art. no. 245201.
[41] A. Phatak, Z. Cheng, C. Qin, and K. Goda, "Design of electro-optic modulators based on graphene-on-silicon slot waveguides," *Opt. Lett.*, vol. 41, no. 11, pp. 2501–2504, 2016.